A THEORETICAL AND PRACTICAL STUDY OF CRACKING OF AN ALUMINIUM ALLOY DURING SIDE PRESSING USING A FINITE-ELEMENT ANALYSIS

D. Salimi-Namin

Department of Mechanical Engineering,
University of Tabriz
Tabriz, Iran

Abstract Elastic-plastic finite-element analysis applied to metalforming allows the real macroscopic properties of the workpiece to be incorporated. This paper presents the results of an experimental study of the initiation of cracking in side-pressing of a heat-treated aluminium alloy (Duralloy 2014). Using an F. E. analysis, these are related to various fracture criteria. It is found that the criterion of generalised plastic work correlates well with the change in fracture site from the centre of the billet to the outer corner as the geometric shape becomes more oblate. For central cracks the limiting deformation is about 13%, but when these are suppressed the deformation can continue to nearly 50%.

چکیده استفاده از روش تحلیلی الاستیکی - پلاستیکی عناصر محدود در مورد روشهای شکل دادن، ما را قادر می سازد تا رفتارهای واقعی و ماکروسکوپیك قطعه کار را مورد بررسی و مطالعه قرار دهیم. این مقاله جمع بندی نتایج حاصل از تجربیاتی است که روی آلیاژ آلومینیم «دورآلوی ۲۰۱۴ Duralloy 2014» برای مطالعه شروع ترك انجام شده است. با بکارگیری روش عناصر محدود و مشخصه های مکانیکی آلیاژ مورد نظر، ملاك های مختلف شروع ترك در فلزات بررسی گردیده است. با مقایسه نتایج نظری حاصل با مشاهدات تجربی، در مورد محل و موقع ظهور ترك، معلوم شد که ملاك «کار پلاستیکی عمومیت داده شده «Generalised Plastic Work» محل ایجاد ترك را، مستقل از شکل هندسی قطعه کار، درست پیش بینی می کند. ولی پیش بینی درست اندازه تغییر شکل لازم برای شروع ترك بستگی بشکل هندسی قطعه کار دارد. در مواردی که ترك در مرکز قطعه کار ظاهر می شود پیش بینی اندازه تغییر شکل برای ظهور ترك، طبق ملاك مزبور، صحیح بوده (از ۱۳ تا ۲۰ درصد برحسب مورد) ولی وقتیکه محل ترك در گوشه خارجی قطعه می باشد اندازه تغییر شکل پلاستیکی لازم برای شروع ترك تا ۵۰٪ نیز می رسد.

INTRODUCTION

Until the present decade, most metal working analysis was confined to the prediction of working loads, and sometimes of the pattern of flow. The assumptions about the materials were crude, usually ignoring strian–hardening, and the geometric conditions that could be handled were highly simplified. The availability of finite - element (F. E.) Plasticity analysis programs has markedly changed the situation [1], especially where three-dimensional problems are concerned [2,3]. Indeed, the scope and detail of the information that can now be obtained raise the problem of performing adequate experimantal tests to compare with the predicted results.

A feature of particular interest and concern in industrial metalworking is the incidence of cracking during processing, especially for certain alloys and certain conditions of heat-treatments. A preliminary survey of this topic [4] has shown clearly that the F.E. method can give valuable predictions of both the location of cracks and the degree of deformation necessary to produce them.

The present study extends the work of Clift et al.[5], using the same simple geometric conditions of plane - strain side - pressing of circular and oblate cylinders, as used also by Kobayashi et al.[6]. The F.E. analysis for this system is well proven and therefore allows comparison of different theories of crack production or initiation. A further check is provided by using a semi - brittle aluminium alloy, Duralloy 2014, in two different conditions of heat - treated stock.

The Finite Element Method and Theoretical Back ground

The «internal work» and «external work» of a field are defined, respectively, by [7]:

$$\text{Wint.} = \int_u \sigma_{ij}\dot{\varepsilon}_{ij}dv,$$

$$\text{Went.} = \int_v F_i u_i dv + \int_s T_i \bar{u}_i ds$$

where F_i is body force per unit volume, T_i is the surface tractions, u_i displacement, σ_{ij} stress vector and ε_{ij} strain vector.

According to the principle of energy balance, a variational formulation, governing the elastic-peastic behavior of materials, can be derived,

$$\phi = \int_v \sigma_{ij}\varepsilon_{ij}dv - \int T_i\bar{u}_i ds - \int F_i u_i dv \qquad (1)$$

Where any heat exchange is ignored.

Expressing this in terms of rate and in equililrium condition we have:

$$\int_v \dot{\sigma}_{ij}\dot{\varepsilon}_{ij}dv \quad \int \dot{T}_i\dot{v}_i ds - \int \dot{F}_i v_i dv = 0 \qquad (2)$$

The distribution of the stress rate vector σ_{ij}, is related with the strain rate vector, ε_{ij}, which in turn is derivable from a continuous velocity vector, v_i.

The body is composed of an isotropic material that obeys Von Mises Yield Criterion and its associated flow rules. The stress rate and strain rate components are associated by Hooke's law in the elastic region and by the Prandtl - Reuss equations during plastic deformation.

For finite element modeling, we have used a mesh divided into quadrilateral elements, interconnected at a finite number of nodal points. This is illustrated, along with nodal point number, geometrical parameters(H and W), in Figure 1(a). We then approximated that the forces acting on the body are concentrated at the nodes of an element, so the variational expression

$$\delta(\dot{d}_{Im})\, f_{Im} = \int \sigma_{ij}\delta(V_{j,i})\, dv \qquad (3)$$

Where f_{Im} is the mth component of force, and d_{Im} the mth component of displacement at node I of the element. The δ symbols in equation (3) denote arbitrary variations in the quantities enclosed in parentheses and integral is taken through the volume of the element. If σ_{ij} in equation (3) is replaced by the Jaumann rate of Cauchy stress [8] the basic rate expression becomes:

$$\delta(d_{Im})\,\dot{f}_{Im} = \int[\delta(\dot{\varepsilon}_{ij})(D_{ijke} - 2\sigma_{ik}\delta_{je})\,\dot{\varepsilon}_{kl} + \delta(V_{j,l})\,\sigma_{ij}V_{j,k}]\, dv \qquad (4)$$

If the deformation increments are kept small, then the fundamental variables like rates of change of nodal displacement, nodal force and particle displacement will be all proportional to their incremental values and equation (4) may be rewritten in an incremental form as:

$$\delta(\Delta d_{Im})\,\Delta f_{Im} = \int \delta(\Delta\varepsilon_{ij})\,(D_{ijkl} - 2\delta_{jl}\sigma_{ik})\,\Delta\varepsilon_{kl} + \delta(u_{j,i})\sigma_{ik}u_{j,k}]\, dv \qquad (5)$$

Where δ_{ij} is the Kronecker delta equating to 1 if i = j, and to zero if i≠j.

During each increment of deformation the stiffness relationship between the applied forces and resulting displacements has the familiar form:

$$\Delta f_{Im} = K_{ImJn}\,\Delta d_{Jn} \qquad (6)$$

In this expression K_{ImJn} is the stiffness matrix and is determined at the midpoint of each increment. For the present finite - element modeling, the stiffness matrix has three components whose detail is explained elsewhere [9].

Theoretical predictions in this work are based on post - processing of the detailed F. E. predictions of the stress and strain in each element, using various criteria for fracture published by a variety of authors. For this purposethe generalized stress and generalized strain were evaluated for each element of the F. E. mesh using the program EPFEM (Elastic - plastic finite - element method) originally produced by Pillinger [2] and subsequently extensively used by others [3, 10]. The actual F.E. program used was that developed by Clift [4] as used in the fracture initiation study quoted [5].

The results were then calculated in a form suitable to the particular criterion to be studied. For example the Generalized Plastic Work (GPW) criterion, first formulated by Freudenthal [11] postulates that cracks will start during deformation when the GPW reaches a critical value, i. e:

$$\int_0^{\bar{\varepsilon}f}\bar{\sigma}d\bar{\varepsilon} = Cl \qquad (7)$$

Where Cl is an empirical constant implicitly containing the volume. More correctly, the criterion should be described as generalized plastic work per unit volume, but this is usually underestood in the definition.

Cockroft and Latham [12] performed tensile tests and concluded that only the tensile plastic work should be included:

$$\int_0^{\bar{\varepsilon}f}\bar{f}(\bar{\sigma})\bar{\tau}d\bar{\varepsilon} = C2 \qquad (8)$$

Brozzo [13] further modified this equation to include an explicit statement of the hydrostatic stress σ_H:

$$\int_0^{\bar{\varepsilon}f}\frac{2\sigma_1}{3(\sigma_1-\sigma_2)}d\bar{\varepsilon} = C3 \qquad (9)$$

Chosh [14] proposed a fracture criterion based upon statistical probabilities of voids joining up by a shear process, following earlier proposals by McClintock et al. [15] and Rice and Tracey [16].

$$(1+\frac{\sigma_2}{\sigma_1})\sigma_1^2 = K \qquad (10)$$

Where K contains various material property inputs.

Another approach was taken by Oyane et al. [17]. This postulates that fracture occurs when the volumetric strain reaches a certain critical value, which is a characteristic of the material:

$$\int_0^{\bar{\varepsilon}f} (1 + \frac{\sigma_m}{a\bar{\sigma}}) \, d\bar{\varepsilon} = C \qquad (11)$$

Where a and C are constants that should be evaluated experimentally. Atkins proposes a further development of the void coalescence theory, in his book [18].

EXPERIMENTAL

The specimens were all produced from Duraloy 2014 aluminium alloy (composition: Al, 3.9-5.0 Cu, 0.5-0.9 Si, 0.5 Fe, 0.4-1.2 Mn, 0.2-0.8 Mg, 0.1 Cr, 0.1 Ni, 0.25 Zn, 0.15 Ti) cylinders, 16mm diameter and 45mm long. Each was cut in half and thefaces were carefully ground flat and perpendicular to the axis. The two halves were held in a constraining container with tightly - fitting shims at one end, so that plane - strain conditions were imposed. The compressive load was then applied transversely to the axis, using flat parallel dies moving slowly at room temperature. The average strain rate was about 0.001 per second to avoid local temperature rise. The specimens were removed at intervals as the load was applied, using smaller intervals as the expected incidence of fracture was approached. Each of the mating surfaces was carefully examined for the appearance of a small visible crack. The presence of a crack can be emphasized by the use of a standard non-destructive testing technique with a fluorescent die penetrant, illuminated by ultraviolet light. A practiced observer with a hand lens can however detect very small cracks (of the order of 1mm long) quite reliably.

Figures 1(a) and 1(b) show the equipment used. The oblate sections were produced by milling accurately flat and parallel areas on diametrically opposite sides of the bar stock. Various ratios, of height H between flats to width W of each flat, were produced for testing. Two heat treatment procedures were followed:

A: Solution treatment for two hours at 500°C followed by water quenching and ageing at room temperature for four days.

B: Solution treatment as in A, followed by ageing at 180°C for 6 hours.

A third heat treatment, annealing.was applied to test the effect of lower strength but higher ductility. As this produced no cracks up to 70% deformation thesetests will not be further discussed here.

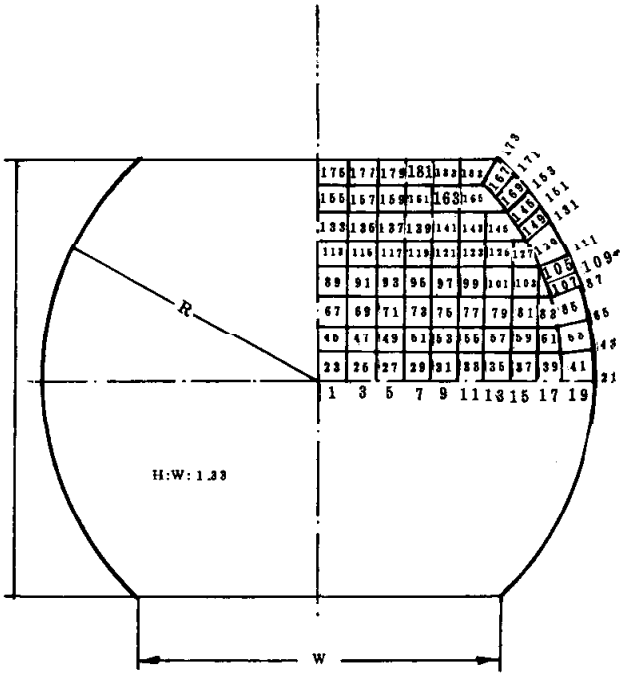

Figure 1(a). Geometric Parameters and Node Numbers of a Mesh.

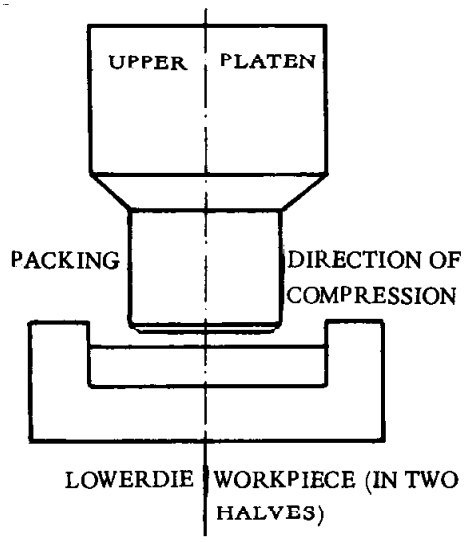

Figure 1(b). Experimental Arrangement for Plain- Stain Side Pressing.

RESULTS

It was first necessary to determine accurately the stress-strain curves for the material. Figure 2 shows the results obtained from a compression test, corrected

to allow for friction [16].

In addition, uniaxial tensile tests were performed to find the strain or work to fracture the specimens. These results are shown in Figure 3.

The cylindrical specimens were then compressed as described and examined for minute cracks. Table 1 shows the sites of the initiation of fracture as predicted by the various theories, with a star grading indicating the degree of agreement with the experimental observations. Figure 4(a) shows the location of the relevant nodes at fracture of the originally circular rod, at 14% height reduction. Fracture occurred at the center, node 2. This may be contrasted with Figure 4(b) where fracture occurred after 49% height reduction near node 174 at the original corner of the billet. This particular initial geometric ratio, H/W= 2.5, is in fact, a transitional one; as Table 1 shows, some fractures occurred at the corner but some at the center.

The feature is clearly seen in Figure 5, which records the percentage deformation at which fracture occurred in the experiments. For all values of H/N from the circular shape (H/W = ∞) down to H/W = 2.5, cracks were found at the center (near node 2), and fracture occurred after about 13% compression. The flatter specimens, however, behaved quite differently. The crack was found near the original corner (near node 174) and did not appear until almost 50% compression had been applied. Table 2 shows that this change of fracture site accords well with the generalized plastic work (GPW) predictions. The remarkable transition at H/W=2.5 is reflected in the low deformation for the specimens of this ratio that failed at the center and the very much larger possible deformation for those nominally identical specimens where the center fracture did not occur, and the sample remained sound until the corner cracked.

A similar pattern of crack location is found with the somewhat more ductile specimens with heat treatment A. This will be discussed in a subsequent publication with reference to the influence of hydrostatic stress on the deformation level at fracture. A comparative result at H/W = 0.577 is given in the last line of Table 2.

The 1.33 ratio specimens came from a batch with lower ducility. Although these failed as predicted at the corner, the precentage deformation at fracture was only 28%.

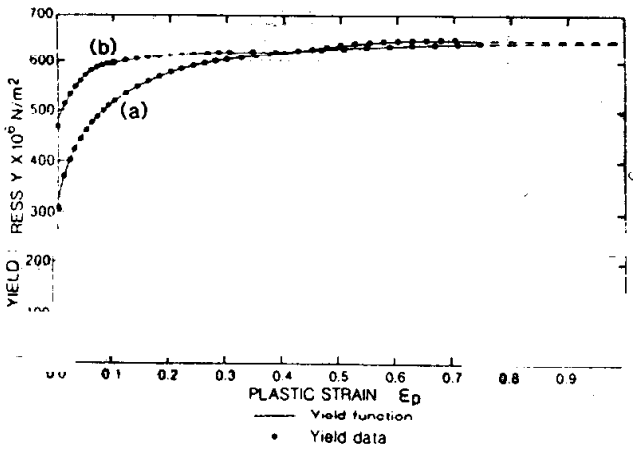

Figure 2. The stress - strain results for Duraloy 2014, aged at room temperature (a) and at 180°C (b)

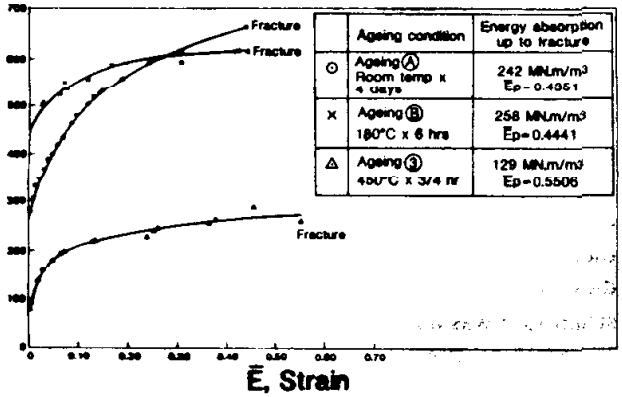

Figure 3. The stress - strain curve for Duraloy 2014, obtained by tensile test, a: room temperature ageing, b: aged at 180°C.

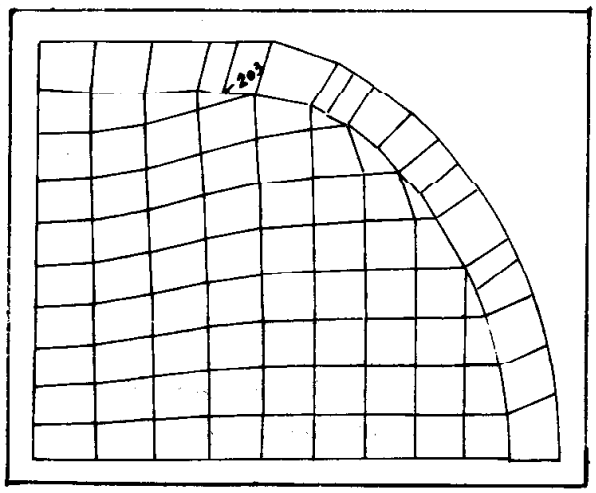

Figure 4(a). The deformed grid of an initially circular section at the stage of crack formation, indicating the location of nodes 2 and 203

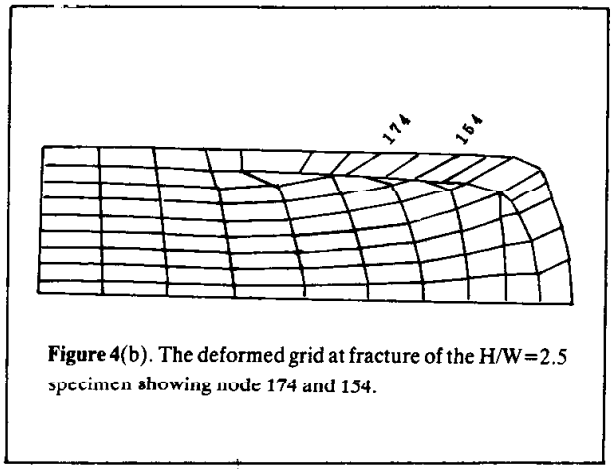

Figure 4(b). The deformed grid at fracture of the H/W=2.5 specimen showing node 174 and 154.

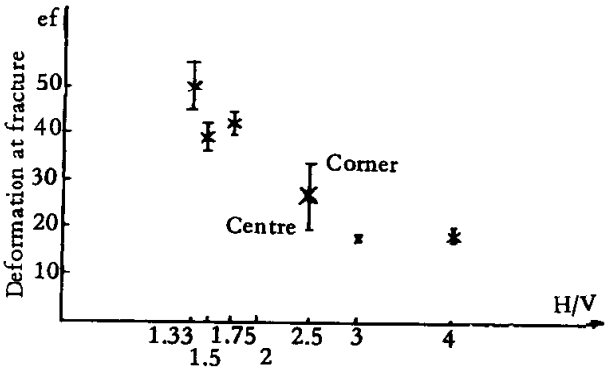

Figure 5 The percentage deformation (reduction in height) at which cracks were first observed for specimens of various H/W ratios. The specimens with H/W = 1.33 were from a batch of lower ductility.

DISCUSSION

These results are in general accord with those produced by Clift[4,5] in showing that cracks may occur either at the center or at the original corner, in side pressing of a cylinder. The crack location is determined primarily by the geometric form, but the metallurgical condition, affecting the ductility, can of course affect the deformation level at which fracture commences.

A striking feature of the present results is the large change in deformation level when the width of the original flats is increased (H/W decreased), as seen in Figure 5.

All specimens from those of circular section down to H/W = 2.5 crack at their centers. It is well known that a tensile stress in the transverse direction is produced by lateral compression of a cylindrical billet, and this is in fact used in some piercing operations to make thick-walled tubes. Nevertheless it should be recognized that the cracks observed in these experiments are not vertical as would be expected from the concept of cracking normal to the maximum tensile stress. They are much closer to a direction of maximum shear [5]. The flatter specimens emphasis this point. The cracks appearing at their corners are clearly not due to a major tensile stress and in all instances follow approximately the direction of maximum shear. In some specimens (H/W = 2.03 and 1.75) the crack appeared along the diagonal, between the center and the corner.

It is suggested that the cracks are predominantly attributable to shearing, and it is consequently expected that the criterion for cracking will be associated with the maximum work of plastic shearing, rather than being directly related to a maximum tensile stress. Table 1 supports this, showing that the fracture site is well predicted by the energy-type theories of GPW, Oyane, Brozzo and Cockcroft, for the high H/W values. There is however a clear change when H/W becomes less than 1.5. Then the Cockcroft theory, which considers only the tensile component of plastic work, is seen to fail, while the other two continue to predict accurately the new fracture site. Brozzo's theory is based on that of Cockcroft and Latham, and this also fails. Atkins' theory is in fact in better agreement for these low H/W values.

The generalized plastic work concept is simple and is to be preferred to Oyane's formulation which is very similar (for non- porous materials) but involves two empirical constants.

The accumulation of plastic work can be studied in more detail with reference to Figure 6(a–c). In Figure 6(a) for the initially circular specimen, the total plastic work is clearly greater for node 2 at all reductions up to about 11%, but 203 subsequently shows more work content. The implication is that if the alloy is sufficiently ductile to survive the early part of the deformation the crack will appear near node 203 rather heat - treatment chosen, fracture occurs at about 13% and is found at the center (node 2).

For the flatter specimens, exemplified by the ratio H/W W=2.5 in Figure 6(b), the total plastic work at node 2 is clearly much greater than that at node 174 (Figure 4(b)), and fracture will again occur at the center. If however the material is sufficiently ductile to allow a deformation of about 30% or more, the node 174 has the greatest work content. As shown in Figure5, this is the transition region where central cracks at low deformation and corner cracks at high deformation are both found experimentally, depending on slight differences in material condition after heat treatment.

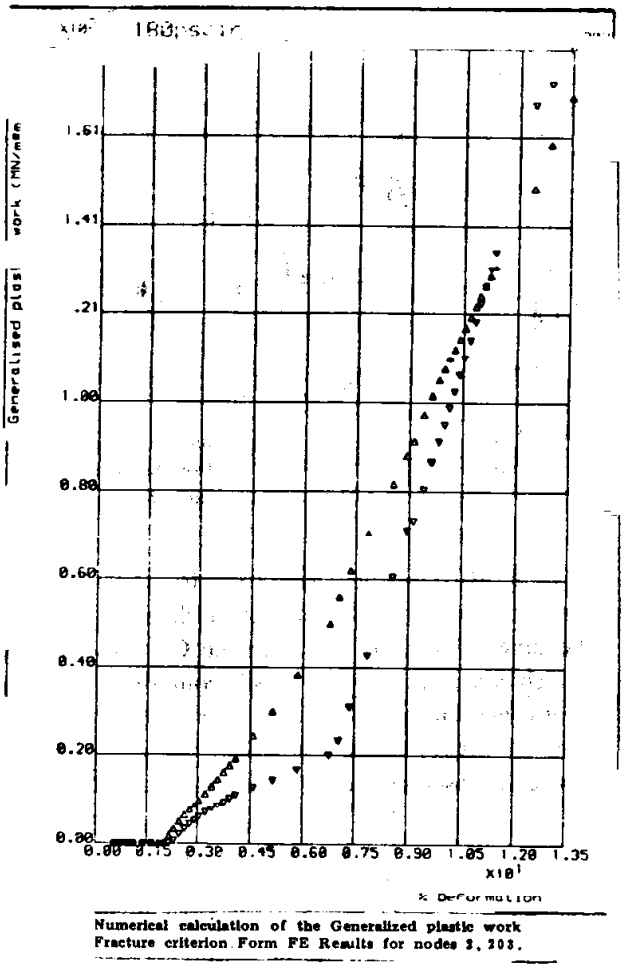

Figure 6. Progressive increase in the generalised plastic work as deformation proceeds, shown for selected relevant nodes: (a) initially cylindrical sample

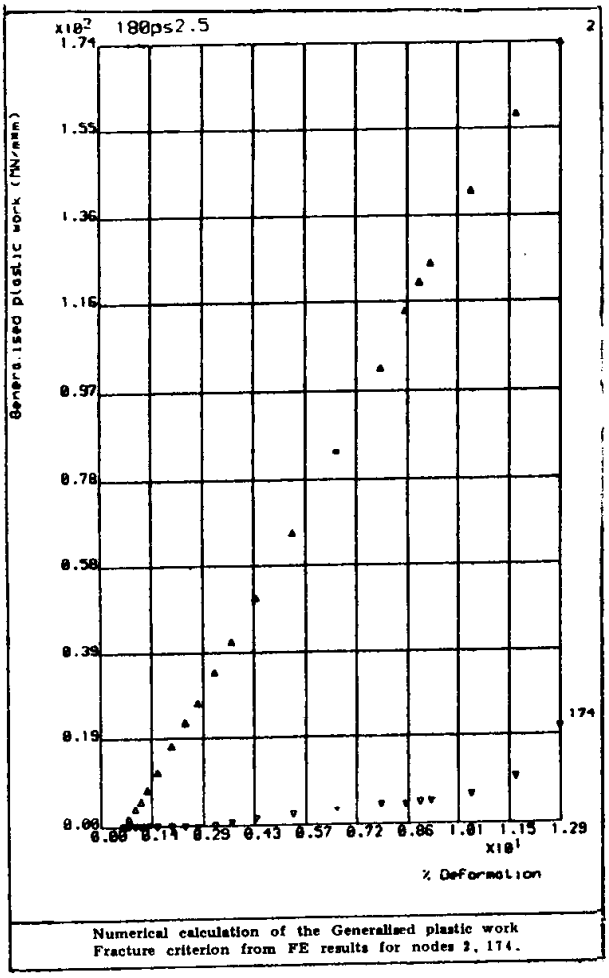

Figure 6(b). H/W=2.5 at low deformation

Although these results are not obviously to be expected, they are not entirely surprising in terms of slip-line field theory, despite the restrictive assumptions made in that theory. For an initially circular cylinder, the field after 20% reduction in height will be as shown in Figure 7 for a further infinitesimal increment.

This will produce a tensile hydrostatic stress at the center as the rigid blocks to left and right move outwards. If however the original H/W ratio is say 2.0, then the rigid zone below the upper punch, after a 20% height reduction, will just reach the center line. Any further reduction will spread the deformation with a plastic central core, so that the stress on the center line intersection becomes compressive.

This may be expected to suppress the fracture deformation can then proceed to a much greater extent before a fracture starts at some other location. Because the deformation is predominantly by shear across the diagonals, a shear crack may be expected somewhere along the major shear band. The original corner is likely to be the most deformed area of the diagonal shear band, because the metal must rotate about the corner as well as shearing.

Although this explanation must be tentative, it provides some background for the agreement of the F. E. predictions with the practical observations. It clearly suggests the extension of this work to alloys of different ductility, such as the specimen with heat-treatments A and B, and to other geometric forms.

It may be expected that such studies will differentiate more clearly between the various crack initiation theories and also elucidate the effect of hydrostatic stress. The post-processing analysis could then by used in conjunction with more complex F. E. analyses to predict fracture in more practical metalforming operations. The work is continuing.

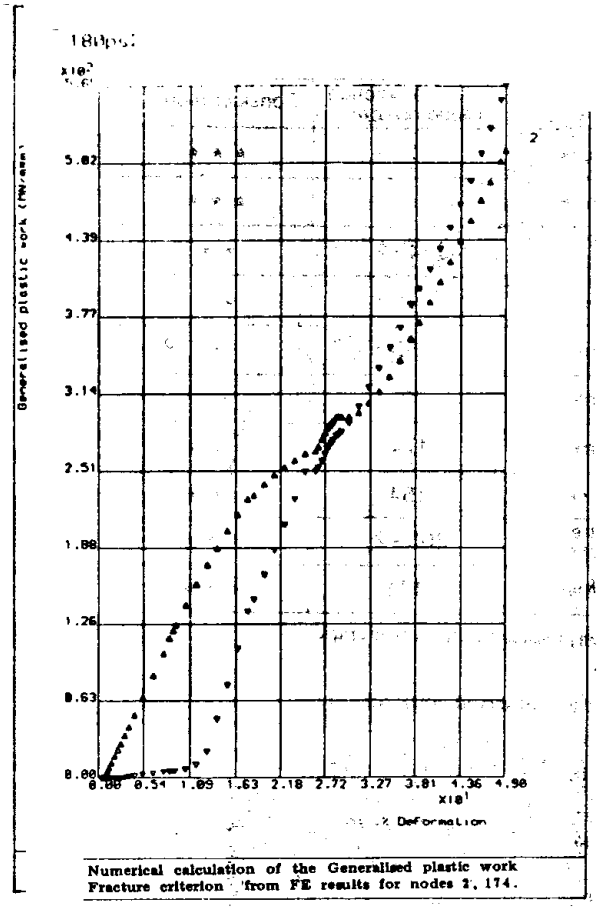

Figure 6(c). H/W=2.5 up to high deformation.

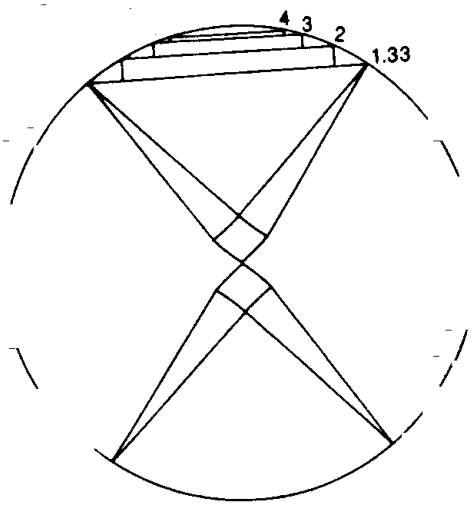

Figure 7. A slip-line field for the initially cylindrical specimen after deformation to 20% reduction in height, which suppresses the central tensile stress.

Table 1. Fracture Sites as Predicted by the Various Theories, Compared with the Experimental Observations.

	G.P.W.		Oyane		Brozzo		Cock & Lath		Atkins		Ghosh	
Specimen	nodes.n	Agreem.	nodes.n	Agreem	nodes.n	Agreem.	nodes.n.	Agreem.	nodes.n.	Agreem.	nodes.n.	Agreem.
25PSCir	1	★ ★ ★	2	★ ★ ★	1	★ ★ ★	2	★ ★ ★	2 210 2	★ ★	22	—
25PS.4	1	★ ★ ★	1	★ ★ ★	1	★ ★ ★	1	★ ★ ★	1 188 1	★ ★	128	—
25PS.3	204	★	2	★ ★ ★	1	★ ★ ★	1	★ ★ ★	203 187 1	★ ★ ★	87	—
25PS2.5	7	★ ★ ★	154	★	7	★ ★ ★	154	★	188 203 151	—	109	—
25PS2.03	189	★ ★	189	★ ★	7	—	153	★ ★	173 112 189	★	154	★ ★
25PS1.75	9	—	122	—	9	—	134	—	9 152 10	★	100	
25PS1.5	174	★ ★ ★	190	★ ★	172	★ ★	2	—	174 171 174	★ ★ ★	173	★ ★ ★
25PS1.33	154	★ ★ ★	46	—	154	★ ★ ★	6	—	153 154 172	★ ★ ★	92	—
180PSCir	203 2	★ ★	2	★ ★ ★	2	★ ★ ★	2	★ ★ ★	216 216 201	—	111	—
180PS1.33	171	★ ★ ★	171	★ ★ ★	2	—	2	—	171 169 171	★ ★ ★	116	—

Table 2. The Percentage Deformation at Which Cracks were Detected for the Various Geometric Initial Shapes, and the GPW Predictions of Sites.

Experimental results

Specimen	Heat T.	H/w	% Exp. frac. def.	Crack site	G.P.W. prediction (node number)	Considerations
25PScir	A	∞	19.84	Centre	1	***
25PS.4	A	4	19.95	Centre	1	***
25PS.3	A	3	18.94	Centre up to near corner	204+2	**
25PS2.5	A	2.5	21.33,N35	Corner & midway between corner & centre	7	**
25PS2.03	A	2.03	50.46	Corner	189	*
25PS1.75	A	1.75	43.0	Corner	9	—
25PS1.5	A	1.5	40.0	Corner	174	***
25PS1.33	A	1.33	50.8	Corner	154	***
180PScir	B	∞	13.37	Centre up to corner	203+2	***
180PS1.33	B	1.33	28.15	Corner	171	***

*** Very good agreement and this when predicted and observed crack sites are located, at the same element

** Good agreement when predicted and observed crack sites are located at the next neiboring elements.

*Poor agreement when the distance between actual crack site and predicted one are two elements apart.

- Non agreement when observed and predicted site of crack are not related to each other at all.

REFERENCES

1. J. F. T. Pittman, O. C. Zienkiewicz, R. D. Wood and J. M. Alexander (eds). «Numerical Analysis of forming Processes» John Wiley, 1984.
2. I. Pillinger, «The prediction of metal flow and properties in three-dimensional forging using the finite element method», PhD Diss., Birmingham, 1984.
3. I. Pillinger, P. Hartley, C. E. N. Sturgess and G. W. Rowe, «An elastic - plastic three - dimensional finite element analysis of the upsetting of rectangular blocks and experimental comparison», Int. J. Mech. Tool Des. Res., 25, 229 - 243, 1985.
4. S. E. Clift, «Identification of defect locations in forged products using the finite - element method», PhD Diss., Birmingham, 1986.
5. S. E. Clift, P. Hartley, C. E. N. Sturgess and G. W. Rowe, «fracture initiations in plane - strain forging» 25th Int. Mach. Tool Des. Res. Conf., 413 - 419, 1985.
6. C. H. Lee and S. Kobayashi, «Analysis of azisymmetric upsetting and plane - strain side - pressing of solid cylinders using the finite - element methods» Trans A. S. M. E. J. Eng. Ind. 96 445 - 454, 1971.
7. P. G. Hodge, Continuum Mechanics, McGraw - Hill, New York, 1970.
8. E. H. Lee, The basis of an Elastic - Plastic code SIDAM Repozt No 76 - 1, Stanford university, CA, 1976.
9. P. Hartley, S. E. Clift, J. Salimi - Namin, C. E. N. Sturgess, I. Pillinger «The prediction of Ductile Fracture initiation in Metalforming using a finite Element Method and Various Fracture criteria», Res Mechanica 28 (1989) 269 - 293.
10. G. W. Rowe, C. E. N. Sturgess, P. Hartley and I. Pillinger, «Finite - element Plasticity and Metalforming Analysis» Camb. U. Press (1987).
11. A. M. Freudenthal, «The inelastic behaviour of engineering materials and structures» J. Wiley, 1950.
12. M. G. Cockcroft and D. J. Latham, «Ductility and Workability of Metals», J. Inst. Met. 96, 33 - 39, 1986.
13. P. Brozzo, B. Deluca and R. Redina «A new method for the prediction of formability limits of metal sheets» in «Sheet metal forming and formability» Proc. 7th Cong. Int. Deep Drg. Gp. 1972.
14. A. K. Ghosh, «A criterion for ductile fracture by the growth of holes», Trans. ASME J. App. Mech. 35, 363, 1976.
15. F. A. McClintock, S. M. Kaplan and C. A. Berg, «Ductile fracture by hole growth in shear bonds» Int. J. Fract. Mech. 2, 614, 1966.
16. J. R. Rice and D. M. Tracey «On the ductile enlargement of voids in triaxial stress fields» J. Mech. Phys. Solids, 17, 201 - 217, 1969.
17. M. Oyane, T. Sato, K. Okimoto and S. Shiam, «Criteria for ductile fracture and their applications» J. Mech. Wkg. Tech. 4, 65 - 81, 1980.
18. A. G. Atkins and Y. W. Mai, «Elastic and Plastic Fracture», Ellis Horwood, Chichester, 1985.
19. G. W. Rowe, «Elements of metalworking theory», Arnold, London, 1979.